Chiral-symmetry restoration at finite densities in Coulomb-gauge QCD

Aleksandar Kocić
Department of Physics, University of Illinois at Urbana-Champaign, 1110 West Green Street, Urbana, Illinois 61801
(Received 29 July 1985)

Using the Schwinger-Dyson equation in the Hartree-Fock approximation, we show that, within a potential model motivated by the QCD Hamiltonian in the Coulomb gauge, chiral symmetry is restored at finite densities. Two cases are studied: a δ-function potential and a linear confining potential. For the former case the phase diagram is obtained analytically, whereas for the latter case numerical techniques are used. The values of physical quantities calculated for the linear confining model are consistently smaller than the experimental ones indicating that a potential with additional short-range attraction is needed to describe the quark interaction in the high-density regime.

I. INTRODUCTION

In heavy-ion collisions nuclei overlap over short time intervals creating high-density matter. The structure of the nucleons becomes important and the many-body aspects of QCD are expected to explain phenomena in this regime. Similar situations leading to high-density matter can be found in neutron stars and in the early Universe. Recent calculations indicate that QCD exhibits a phase transition at finite temperatures and densities.[1] Deconfinement and chiral-symmetry restoration occur leading to a new phase of matter: the quark-gluon plasma.

Calculations have been done by using perturbation theory and lattice simulation to locate both transitions.[1,2] Perturbative analysis is unfortunately limited to densities much higher than those expected to give the transition and convergence of the perturbation series does not seem to be good enough to make reliable extrapolations. Lattice simulations give accurate predictions only in the high-temperature regime because the inverse temperature determines the lattice size in the temporal direction. Low temperatures require larger lattices and finite-size effects produce sizable uncertainties. Furthermore, the inclusion of fermions on a lattice is still problematic. Because of these difficulties the relation between chiral-symmetry restoration and deconfinement is still unclear and it is important to investigate other possibilities of describing this regime of QCD.

In this paper chiral-symmetry restoration at zero temperature and finite densities will be studied within the framework of a potential model recently proposed by Finger and co-workers.[3]

The accepted picture of the chiral-symmetry-breaking mechanism is that for sufficiently strong couplings the perturbative vacuum is unstable against the formation of quark-antiquark bound states.[4] The physical ground state is a quark pair condensate and it transforms in a nontrivial way under the chiral group. The presence of surrounding quarks induces a shift in the energy of a quark-antiquark bound state which is negative relative to an empty state. This shift is due partly to the interaction between the surrounding quarks and those in the condensate and partly to Pauli blocking. Increasing the density will diminish the strength of the interaction and eventually the symmetric vacuum will be stabilized leading to chiral-symmetry restoration.

In Sec. II we will review the model. In Sec. III the generalization to finite temperatures and densities will be given. In order to gain some intuition about the nature of the phase transition, a simple example of a δ-function potential will be worked out in detail in Sec. IV. This model is not realistic, only pedagogical. Numerical solutions and results for the confining potential are presented in Sec. V. In Sec. VI relevant conclusions are drawn and we discuss the limitations of the model and its possible extensions and improvements.

II. REVIEW OF THE MODEL

Recently it was shown that in the Coulomb gauge the QCD Hamiltonian can be written as[3]

$$H=\int d^3x\,\psi^\dagger(x)(-i\boldsymbol{\alpha}\cdot\nabla)\psi(x) + \tfrac{1}{2}\int d^3x\int d^3y\,\rho^a(x)\left[\frac{4\pi\alpha}{\nabla^2}\right](x,y)\rho^a(y) + \text{transverse gauge}\,, \tag{2.1}$$

where

$$\rho^a=\psi^\dagger\frac{\lambda^a}{2}\psi \tag{2.2}$$

and $\lambda^a/2$ are generators of the SU(N) color group in the fundamental representation.

Motivated by the fact that quarks are the relevant degrees of freedom responsible for chiral-symmetry breaking, we restrict our analysis to the quark sector of the theory's Fock space. In this case the "transverse gauge" part of the Hamiltonian (2.1) does not enter the calculations and one can work with the effective Hamiltonian

$$H_{\text{eff}}=\int d^3x\,\psi^\dagger(x)(-i\boldsymbol{\alpha}\cdot\nabla)\psi(x) + \tfrac{1}{2}\int d^3x\int d^3y\,\rho^a(x)\left[\frac{4\pi\alpha}{\nabla^2}\right](x,y)\rho^a(y)\,. \tag{2.3}$$

This procedure of dropping terms in Eq. (2.1) is discussed in greater detail in Ref. 3.

The fermion gap equation obtained from $H_{\rm eff}$ corresponds to the instantaneous ladder approximation of the Bethe-Salpeter kernel. This approximation is used in the phenomenological treatment of heavy quarkonia and the structure of $H_{\rm eff}$ admits the immediate generalization to phenomenological potentials.

It is believed that the ground state of the strongly coupled QCD is a quark pair condensate. The pairing mechanism is very similar in nature to the formation of Cooper pairs in the theory of superconductivity and this analogy has been exploited since the idea of spontaneous chiral-symmetry breaking was first introduced by Nambu and Jona-Lasinio.[5]

In the potential model we want to study, the ground state is determined variationally starting with the BCS-type ansatz[3,5]

$$|\psi\rangle=\frac{1}{N[\psi]}\exp\left[\sum_s\int d^3p\, s\psi_p b_i^\dagger(\mathbf{p},s)d_i^\dagger(-\mathbf{p},s)\right]|0\rangle\ , \tag{2.4}$$

where $|0\rangle$ is an empty state and $b_i^\dagger(\mathbf{p},s)$ and $d_i^\dagger(-\mathbf{p},s)$ are quark and antiquark creation operators, respectively, with momentum $\mathbf{p}$, helicity s, and color i. The flavor indices have been suppressed.

The trial function ψ_p is determined from the extremum condition

$$\frac{\delta}{\delta\psi_p}\langle\psi|H_{\rm eff}|\psi\rangle=0 \tag{2.5}$$

and the normalization constant is fixed by requiring

$$\langle\psi|\psi\rangle=1\ . \tag{2.6}$$

The quarklike excitations of the ground state (2.4) are created by

$$B_i^\dagger(\mathbf{p},s)=\frac{1}{(1+\psi_p{}^2)^{1/2}}[b_i^\dagger(\mathbf{p},s)+s\psi_p d_i(-\mathbf{p},s)]\ , \tag{2.7a}$$

$$D_i^\dagger(-\mathbf{p},s)=\frac{1}{(1+\psi_p{}^2)^{1/2}}[d_i^\dagger(-\mathbf{p},s)-s\psi_p b_i(\mathbf{p},s)]\ . \tag{2.7b}$$

The transformation from (b,d) to (B,D) is the Bogoliubov-Valatin transformation[3] and we shall refer to the excitations represented by $B^\dagger$ and $D^\dagger$ as pseudoparticles or dressed quarks.

The equivalent approach to the calculation of a ground state and a quark self-energy is to solve the Schwinger-Dyson (SD) equation in the Hartree-Fock approximation. This will prove to be the more convenient approach because it admits a straightforward extension to the case of finite temperatures and densities. Derivations in the next section will be done for a general potential $V(x)$.

III. SCHWINGER-DYSON EQUATION AT FINITE TEMPERATURES AND DENSITIES

For the effective Hamiltonian in (2.3), the equation for the quark self-energy is represented in Fig. 1. The

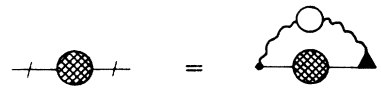

FIG. 1. Schwinger-Dyson equation for the quark self-energy. The hatched circle is the proper self-energy; the open circle is the screened potential, and the hatched triangle is the full vertex.

Hartree-Fock approximation consists in replacing the screened potential and the full vertex by their bare values, Fig. 2. The Hartree term, Fig. 3, vanishes because SU(N) generators are traceless.

In the imaginary-time formalism the fermion propagator is[6]

$$S_{\alpha\beta}(\mathbf{x}\mathbf{x}'|\tau\tau')=-\mathrm{Tr}\{\rho T_\tau[\psi_\alpha(\mathbf{x}\tau)\bar\psi_\beta(\mathbf{x}'\tau')]\}\ , \tag{3.1}$$

where

$$\rho=\frac{e^{-\beta(H-\mu N)}}{\mathrm{Tr}e^{-\beta(H-\mu N)}}\ , \tag{3.2}$$

where

$$\beta=\frac{1}{T}\ . \tag{3.3}$$

Quark fields satisfy antiperiodic boundary conditions in the τ direction with period β. The propagator (3.1) is diagonal in color and flavor indices and this dependence will be suppressed. In terms of S, the equation in Fig. 2 can be written as

$$\Sigma(p)=C_F\int_q\tilde V(p-q)\gamma^0S(q)\gamma^0\ , \tag{3.4}$$

with fermion propagator

$$S(q)=\frac{1}{q-\Sigma(q)}\ , \tag{3.5}$$

where

$$q_0=i\omega_n+\mu\ . \tag{3.6}$$

$\tilde V(k)$ is the Fourier transform of the potential, C_F is the Casimir operator in the fundamental representation of SU(N) color group, $\Sigma(p)$ is the quark self-energy, and $\int_q$ stands for the integration over the three-momenta together with summation over the discrete frequencies

$$\omega_n=\frac{2n+1}{2}\frac{\pi}{\beta}\ . \tag{3.7}$$

Since the interaction is instantaneous, $\tilde V(k)$ depends on $|\mathbf{k}|$ only. As a consequence, $\Sigma(p)$ is ω_n independent and the frequency sum in (3.4) can be performed easily. The quark propagator has to be defined for this case as

$$S_{\alpha\beta}(x,x')=\lim_{\tau\to\tau'}\tfrac{1}{2}\langle[\psi_\alpha(x\tau),\bar\psi_\beta(x'\tau')]\rangle\ . \tag{3.8}$$

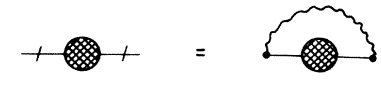

FIG. 2. SD equation in the Hartree-Fock approximation.

The general form of $\Sigma(p)$ is then

$$\Sigma(\mathbf{p})=a_p+b_p\mathbf{p}\cdot\boldsymbol{\gamma}+c_p\gamma^0 , \tag{3.9}$$

where the functions a_p, b_p, and c_p depend on $|\mathbf{p}|$. Fourier transforming (3.8), we find

$$S(\mathbf{p})=-\frac{1}{2\beta}\sum_n[e^{-i\omega_n\eta}S(p\,|\,\omega_n)+e^{i\omega_n\eta}S(p\,|\,\omega_n)] , \tag{3.10}$$

where the limit $\eta\to 0^+$ is understood. Using

$$\sum_n e^{i\omega_n\eta}\frac{1}{i\omega_n-x}=\frac{\beta}{e^{\beta x}+1} \tag{3.11}$$

and

$$\sum_n e^{-i\omega_n\eta}\frac{1}{i\omega_n-x}=-\frac{\beta}{e^{-\beta x}+1} , \tag{3.12}$$

it is straightforward to obtain $S(\mathbf{p})$ which can be rewritten as

$$S(\mathbf{p})=-\frac{1}{2\beta}\sum_n e^{i\omega_n\eta}\left[S(\mathbf{p}\,|\,\omega_n)+S\left[\mathbf{p}\,\middle|\,\frac{2\pi}{\beta}-\omega_n\right]\right] . \tag{3.13}$$

Define the pseudoparticle energy

$$\omega_p=[a_p{}^2+(1+b_p)^2p^2]^{1/2} , \tag{3.14a}$$

shifted chemical potential

$$\nu_p=\mu-c_p \tag{3.14b}$$

and Dirac Hamiltonian

$$H_{\mathbf{p}}=\gamma^0a_p+(1+b_p)\gamma^0\mathbf{p}\cdot\boldsymbol{\gamma} . \tag{3.14c}$$

In terms of these quantities, the quark propagator is

$$S(\mathbf{p}\,|\,\omega_n)=\frac{(i\omega_n+\nu_p)\gamma^0+H_p\gamma^0}{(i\omega_n+\nu_p)^2+\omega_p{}^2} . \tag{3.15}$$

Applying (3.11) and (3.12) we obtain

$$S(\mathbf{p})=\frac{H_p}{2\omega_p}\gamma^0(1-n_p-\bar{n}_p)-\frac{\gamma^0}{2}(n_p-\bar{n}_p) , \tag{3.16}$$

with occupation number for fermions

$$n_p=\frac{1}{e^{\beta(\omega_p-\nu_p)}+1} \tag{3.17a}$$

and antifermions

$$\bar{n}_p=\frac{1}{e^{\beta(\omega_p+\nu_p)}+1} . \tag{3.17b}$$

The overall Fermi factor $1-n_p-\bar{n}_p$ will appear often so we denote it by F_p

$$F_p=1-n_p-\bar{n}_p . \tag{3.18}$$

As a function of T and μ, F_p has the following limiting behavior:

$$F_p(0,0)=1 , \tag{3.19a}$$

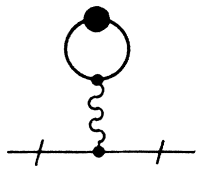

FIG. 3. Hartree term for the quark self-energy.

$$F_p(T,0)=\tanh\left[\frac{\beta\omega_p}{2}\right] , \tag{3.19b}$$

$$F_p(0,\mu)=\theta(\omega_p-\nu_p) . \tag{3.19c}$$

The Schwinger-Dyson equation (3.4) now can be written in terms of functions a_p, b_p, and c_p:

$$a_p+b_p\mathbf{p}\cdot\boldsymbol{\gamma}+c_p\gamma^0 =\frac{C_F}{2}\int_q\tilde{V}(\mathbf{p}-\mathbf{q})\left[F_q\frac{a_q+(1+b_q)\mathbf{q}\cdot\boldsymbol{\gamma}}{\omega_q}-\gamma^0(n_q-\bar{n}_q)\right] , \tag{3.20}$$

and from now on

$$\int_q=\int\frac{d^3q}{(2\pi)^3} . \tag{3.21}$$

This becomes a system of three coupled equations

$$a_p=\frac{C_F}{2}\int_q\tilde{V}(\mathbf{p}-\mathbf{q})F_q\frac{a_q}{\omega_q} , \tag{3.22a}$$

$$(1+b_p)p=p+\frac{C_F}{2}\int_q\tilde{V}(\mathbf{p}-\mathbf{q})F_q\frac{(1+b_q)q}{\omega_q}\hat{\mathbf{p}}\cdot\hat{\mathbf{q}} , \tag{3.22b}$$

$$c_p=-\frac{C_F}{2}\int_q\tilde{V}(\mathbf{p}-\mathbf{q})(n_q-\bar{n}_q) . \tag{3.22c}$$

The first two equations can be rewritten in terms of the Bogoliubov angle ϕ_p defined by

$$a_p=\omega_p\sin\phi_p , \tag{3.23a}$$

$$(1+b_p)p=\omega_p\cos\phi_p . \tag{3.23b}$$

The trial function ψ_p and the angle ϕ_p are related by

$$\sin\phi_p=\frac{2\psi_p}{1+\psi_p{}^2} , \tag{3.24a}$$

$$\cos\phi_p=\frac{1-\psi_p{}^2}{1+\psi_p{}^2} , \tag{3.24b}$$

$$\psi_p=\tan(\phi_p/2) . \tag{3.24c}$$

In terms of ϕ_p Eqs. (3.22) become

$$p\sin\phi_p=\frac{C_F}{2}\int_q\tilde{V}(\mathbf{p}-\mathbf{q})F_q(\sin\phi_q\cos\phi_p-\sin\phi_p\cos\phi_q\hat{\mathbf{p}}\cdot\hat{\mathbf{q}}) , \tag{3.25a}$$

$$\omega_p=p\cos\phi_p+\frac{C_F}{2}\int_q\tilde{V}(\mathbf{p}-\mathbf{q})F_q(\sin\phi_q\sin\phi_p+\cos\phi_q\cos\phi_p\hat{\mathbf{p}}\cdot\hat{\mathbf{q}}) \tag{3.25b}$$

and the equation for c_p is left unchanged.

It remains to solve the system (3.25) together with (3.22c). The quark energy in the expression for n_p and $\bar{n}_p$ depends on temperature and density so the three equations need to be treated self-consistently. Once the solution to the gap equation (3.25a) is obtained, the quark propagator is known and relevant physical quantities can be calculated.

IV. A SIMPLE EXAMPLE: δ-FUNCTION POTENTIAL

Before attempting to solve the gap equation (3.25a) for a confining potential, it is useful to study a phase diagram of a simple, exactly solvable model: the δ-function potential. The reason we choose this example is the simplicity rather than its physical significance. In three dimensions, a δ function produces short-distance singularities in most physical quantities so, to regulate the integrals, we shall restrict the phase space inside the sphere

$$|\mathbf{p}| \leq \Lambda , \tag{4.1}$$

where Λ will be assumed large. In coordinate space, this corresponds to a short-distance cutoff:

$$r_0 \sim \frac{2\pi}{\Lambda} . \tag{4.2}$$

It will be shown, that for the particular values of coupling constant considered here, the results are insensitive to the cutoff procedure.

For the potential

$$\tilde{V}(q)=g \tag{4.3}$$

the gap equation (3.25a) becomes

$$p \sin\phi_p = \frac{C_F g}{2} \int_q F_q \sin\phi_q \cos\phi_p , \tag{4.4}$$

where the cutoff $\theta(\Lambda-q)$ is understood in all the integrals. The p-independent part on the right-hand side of (4.4) is the mass gap of the quark

$$\Delta = \frac{C_F g}{2} \int_q F_q \sin\phi_q . \tag{4.5}$$

This identification is immediately justified because Eq. (4.4) becomes

$$\tan\phi_p = \frac{\Delta}{p} \tag{4.6}$$

and the quark energy is

$$\omega_p = (p^2+\Delta^2)^{1/2} . \tag{4.7}$$

Hence, the gap equation reduces to

$$\Delta = \frac{C_F g}{2} \int_q F_q \frac{\Delta}{(q^2+\Delta^2)^{1/2}} . \tag{4.8}$$

Function c_p of Eq. (3.22c) is independent of p

$$c = -\frac{C_F g}{2} \int_q (n_q - \bar{n}_q) \tag{4.9}$$

or, using the definition of the quark density

$$n = 2N_c n_f \int_q (n_q - \bar{n}_q) , \tag{4.10}$$

$$c = -\frac{C_F g}{4N_c n_f} n . \tag{4.11}$$

At zero temperature and density, Eq. (4.8) has two solutions: $\Delta_0=0$ and $\Delta_0\neq 0$. For a given $\Delta_0\neq 0$,

$$1 = \frac{C_F g}{2} \int_q \frac{1}{(q^2+\Delta^2)^{1/2}} \tag{4.12}$$

places a constraint on the coupling constant g which has to exceed some critical value g_c with g_c given by

$$1 = \frac{C_F g_c}{2} \int_q \frac{1}{q} \tag{4.13}$$

or

$$\frac{C_F g_c}{8\pi^2} = \frac{1}{\Lambda^2} . \tag{4.14}$$

Using this relation it will be possible to trade Λ^2 for g_c in subsequent calculations. From now on, g will be fixed and greater than g_c. A critical line in a (T,ν) or (T,n) plane will be determined by solving (4.8) in the limit $\Delta \to 0^+$.

Two limiting cases are extremely easy to obtain.

(i) $T=0$, $n\neq 0$.

$$F_q = \theta(q-p_F) , \tag{4.15}$$

where p_F is defined by

$$(p_F{}^2+\Delta^2)^{1/2} = \nu , \tag{4.16}$$

and

$$\nu = \mu - c . \tag{4.17}$$

As $\Delta \to 0$, $p_F \to \nu$. At critical density Δ vanishes and the chemical potential approaches its critical value ν_c given by

$$1 = \frac{C_F g}{2} \int_q \theta(q-\nu_c) \frac{1}{q} . \tag{4.18}$$

Note that

$$\theta(q-\nu_c) = 1 - \theta(\nu_c - q) \tag{4.19}$$

so that (4.18) becomes

$$1 = \frac{C_F g}{2} \int_q \frac{1}{q} - \frac{C_F g}{2} \int_q \theta(\nu_c - q) \frac{1}{q} . \tag{4.20}$$

Using the definition of g_c we arrive at

$$\nu_c{}^2 = \frac{8\pi^2}{C_F} \frac{g-g_c}{g g_c} . \tag{4.21}$$

The corresponding density is

$$n_c = \frac{N_c n_f}{3\pi^2} \nu_c{}^3 . \tag{4.22}$$

(ii) $T\neq 0$, $n=0$.

In this case, the gap equation has the form

$$1 = \frac{C_F g}{2} \int_q \frac{1}{q} \left[1 - \frac{2}{e^{\beta_c q}+1} \right] . \tag{4.23}$$

Since the second term on the right-hand side of (4.23) is rapidly converging for large q, we can extend the limits of integration to infinity

$$\int_0^\infty dq\, q \frac{2}{e^{q/T_c}+1} = \frac{\pi^2 T_c^2}{6} . \tag{4.24}$$

Hence, (4.23) results in

$$\frac{\pi T_c}{\sqrt{3}} = \nu_c . \tag{4.25}$$

In the general case of finite temperature and density, a critical line is given by

$$\frac{g}{g_c} - 1 = \frac{C_F g}{4\pi^2} \int_0^\infty dq\, q \left[\frac{1}{e^{(q-\nu)/T}+1} + \frac{1}{e^{(q+\nu)/T}+1} \right] . \tag{4.26}$$

Evaluating the integral

$$\int_0^\infty dq\, q \left[\frac{1}{e^{(q-\nu)/T}+1} + \frac{1}{e^{(q+\nu)/T}+1} \right] = \frac{1}{2} \left[\nu^2 + \left[\frac{\pi T}{\sqrt{3}} \right]^2 \right] , \tag{4.27}$$

Eq. (4.26) simplifies to

$$\nu_c^2 = \nu^2 + \left[\frac{\pi T}{\sqrt{3}} \right]^2 . \tag{4.28}$$

The corresponding phase diagram in the (T,ν) plane is sketched in Fig. 4.

To obtain the (T,n) diagram, we calculate the fermion density for $\Delta \to 0^+$:

$$n = 2N_c n_f \int_q \left[\frac{1}{e^{(q-\nu)/T}+1} + \frac{1}{e^{(q+\nu)/T}+1} \right] \tag{4.29}$$

or

$$n = \frac{N_c n_f}{\pi^2} \nu \left[\frac{\nu^2}{3} + \left[\frac{\pi T}{\sqrt{3}} \right]^2 \right] . \tag{4.30}$$

Substituting for ν from Eq. (4.28) gives

$$n = \frac{n_f N_c}{3\pi^2} (\nu_c^2 - \tau^2)^{1/2} (\nu_c + 2\tau^2) , \tag{4.31}$$

with

$$\tau = \frac{\pi T}{\sqrt{3}} . \tag{4.32}$$

It is convenient to rescale n with n_c given in Eq. (4.22):

$$n/n_c = [1-(\tau/\nu_c)^2]^{1/2} [1+2(\tau/\nu_c)^2] . \tag{4.33}$$

The phase diagram is given in Fig. 5. The energy density difference is positive definite and the transition is second order along the entire line.

As we mentioned earlier in this section, the validity of our results has to be justified by showing that the average length scale in this problem is much bigger than the cutoff r_0. We have to demonstrate two things:

$$n \ll \Lambda^3 \tag{4.34}$$

and

$$\rho \ll \Lambda^3 , \tag{4.35}$$

where ρ is the scale associated with the condensate and represents the density of pairs in the condensate. It is defined as

$$\rho = 2N_c n_f \int_q F_q \left[\frac{1-\cos\phi_q}{2} \right] \tag{4.36}$$

and it has a maximum at zero temperature and density.

Equations (4.34) and (4.35) give

$$\frac{g-g_c}{g} \ll 1 \tag{4.37}$$

and

$$\Delta_0 \ll \Lambda . \tag{4.38}$$

As a final remark to this model we calculate the pion-decay constant f_π. The detailed derivation has been done by Govartes, Mandula, and Weyers,[7] so we just state the final results. For a general potential

$$g(p)\omega_p = \sin\phi_p + \frac{C_F}{2} \int_q \tilde{V}(\mathbf{p}-\mathbf{q}) F_q (\sin\phi_p \sin\phi_q + \cos\phi_p \cos\phi_q \hat{\mathbf{p}}\cdot\hat{\mathbf{q}}) g(q) , \tag{4.39}$$

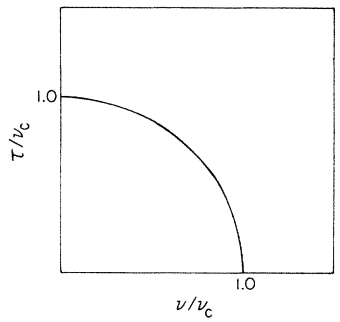

FIG. 4. Critical line in the temperature—chemical-potential plane.

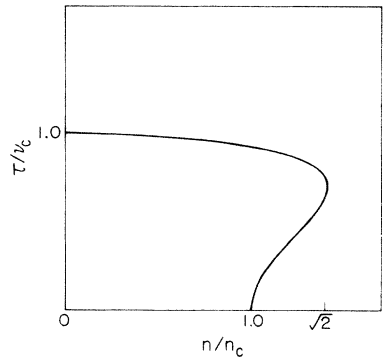

FIG. 5. Critical line in the temperature-density plane.

where

$$g(p)=\frac{\bar{P}(p)}{\omega_p{}^2} \tag{4.40}$$

and $\bar{P}(p)$ is a pion-vertex-part form factor. Normalization of $g(p)$ is

$$f_\pi{}^2=N_c\int_q F_q\sin\phi_q g(q)\ . \tag{4.41}$$

For the δ-function potential at zero temperature and density

$$g(p)=\left[1+\frac{C_F g}{2}\int_q \sin\phi_q g(q)\right]\frac{\sin\phi_p}{\omega_p} \tag{4.42}$$

or using the notation

$$\gamma=1+\frac{C_F g}{2}\int_q \sin\phi_q g(q)\ , \tag{4.43}$$

$$g(p)=\gamma\frac{\sin\phi_p}{\omega_p} \tag{4.44}$$

and

$$f_\pi{}^2=\frac{2N_c}{C_F g}(\gamma-1)\ . \tag{4.45}$$

To leading order in Δ_0/Λ

$$\frac{1}{\gamma}=1+\frac{C_F g}{8\pi^2}\Delta_0{}^2-2\frac{g-g_c}{g_c}\ . \tag{4.46}$$

So

$$f_\pi{}^2=\frac{N_c}{2\pi^2}\left[\nu_c{}^2-\frac{\Delta_0{}^2}{2}\right] \tag{4.47}$$

or

$$\nu_c{}^2=\frac{2\pi^2}{N_c}f_\pi{}^2+\frac{\Delta_0{}^2}{2}\ . \tag{4.48}$$

Finally, we can relate g and g_c:

$$g=\frac{g_c}{1-\frac{C_F g_c}{8\pi^2}\left[\Delta_0{}^2/2+\frac{2\pi^2}{N_c}f_\pi{}^2\right]}\ . \tag{4.49}$$

This justifies the requirement (4.37) and the whole system is consistent with the assumption that the relevant scale in this problem is much bigger than the cutoff distance.

V. GAP EQUATION FOR THE CONFINING POTENTIAL

Previous calculations related to this model indicated that no chiral-symmetry restoration occurs at finite temperature for the case of a purely confining interaction.[8] This is understood easily from the fact that for fixed string tension, quarks remain confined permanently because the thermal energy never exceeds the binding one. Furthermore, the gluon dynamics is neglected in this model, apart from the conjecture that it produces the confining potential between two quarks so the string tension does not develop the proper temperature dependence.[9] Hence, the chiral-symmetry restoration cannot occur without deconfinement.

At zero temperature and finite density, the nature of the chiral transition is different. It was pointed out recently[10] that the self-energy of confined quarks is a triggering mechanism for chiral-symmetry breaking. It is negative and infrared singular so its main contribution comes from the low-momentum region. The presence of additional quarks above the filled Fermi sea makes this region unavailable and, as the quark density increases, the effect of the self-energy weakens leading eventually to chiral-symmetry restoration.

In this section we pursue the calculations of the gap equation at zero temperature and finite densities for a purely confining potential

$$V(r)=-\sigma r\ . \tag{5.1}$$

Calculations will be done numerically and the gap function will be evaluated for different densities. In this case, the Fermi distribution factors defined in Sec. III, Eqs. (3.17)—(3.19) reduce to

$$n_p=\theta(p_F-p)\ , \tag{5.2a}$$

$$\bar{n}_p=0\ , \tag{5.2b}$$

$$F_p=\theta(p-p_F)\ , \tag{5.2c}$$

and the Fermi momentum p_F is defined by

$$\omega_{p_F}=\nu_{p_F}\ . \tag{5.3}$$

Hence, the gap equation becomes

$$p\sin\phi_p=\frac{C_F}{2}\int_q \tilde{V}(\mathbf{p}-\mathbf{q})\theta(q-p_F)\times(\sin\phi_q\cos\phi_p-\sin\phi_p\cos\phi_q\hat{\mathbf{p}}\cdot\hat{\mathbf{q}})\ . \tag{5.4}$$

The fermion density at zero temperature is

$$n=2N_c n_f\int_q\theta(p_F-q) \tag{5.5a}$$

or

$$n=\frac{N_c n_f}{3\pi^2}p_F{}^3\ . \tag{5.5b}$$

For completeness, we rewrite the expressions for the order parameter and the density of pairs in the condensate

$$\langle\bar{\psi}\psi\rangle=-2N_c\int_q\theta(q-p_F)\sin\phi_q\ , \tag{5.6}$$

$$\rho=2N_c n_f\int_q\theta(q-p_F)\left[\frac{1-\cos\phi_p}{2}\right]\ . \tag{5.7}$$

The gap equation is free of infrared divergences and we can use

$$\tilde{V}(\mathbf{k})=\frac{8\pi\sigma}{(\mathbf{k}^2)^2} \tag{5.8}$$

as a Fourier transform of the potential (5.1). In fact, we can use (5.8) for the calculations of all the quantities that represent color singlets.[8,11] The angular integration in (5.4) can be performed analytically and the problem reduces to a one-dimensional nonlinear integral equation:

$$p\sin\phi_p=\frac{2C_F\sigma}{\pi}\int_{p_F}^{\infty}dq\,q^2\left[\frac{\sin\phi_q\cos\phi_p}{(p^2-q^2)^2}+\left[\frac{p^2+q^2}{2pq}\frac{1}{(p^2-q^2)^2}-\frac{1}{4p^2q^2}\ln\left|\frac{p+q}{p-q}\right|\right]\sin\phi_p\cos\phi_q\right] . \tag{5.9}$$

Before solving this equation, we have to handle the apparent singularity of the integrand in (5.9) at $q=p$. Both the numerator and denominator on the right-hand side vanish at that point producing a finite limit. Hence, it is convenient to separate the integration interval (p_F,∞) into two parts: one containing a small neighborhood of p and the other containing the rest. In this way, Eq. (5.9) has a general form

$$K_p[\phi]\sin\phi_p+L_p[\phi]\cos\phi_p+M_p[\phi]\sin\phi_p\cos\phi_p=0 , \tag{5.10}$$

where K, L, and M are functionals of ϕ.

This is solved iteratively using the Gauss-Seidel algorithm as suggested[11,12] in Ref. 11. To start with a good ansatz, it is necessary to have a correct asymptotic form of the solution.

At $p=0$,

$$\phi(0)=\frac{\pi}{2} . \tag{5.11}$$

As $p\to\infty$,

$$p\sin\phi_p\to\frac{C_F}{4\pi^2}\tilde{V}(p)\int_0^{\infty}dq\,q^2\theta(q-p_F)\sin\phi_q , \tag{5.12}$$

or recalling the definition of $\langle\bar{\psi}\psi\rangle$,

$$\sin\phi_p\to\frac{C_F}{4N_c}|\langle\bar{\psi}\psi\rangle|\frac{\tilde{V}(p)}{p} . \tag{5.13}$$

Note that, since Eq. (5.10) is nonlinear, the coefficient in (5.13) is important. The string tension sets the scale in this problem and the transformation

$$p\to p/\sqrt{\sigma} \tag{5.14}$$

makes σ disappear from the gap equation.

The form of the gap function ψ_p for several values of Fermi momenta is illustrated in Fig. 6. For each value of p_F, the solution of the gap equation was used to calculate the order parameter (Fig. 7). It was found that for $p_F/\sqrt{\sigma}\geq 0.13$, the only solution is $\psi_p=0$ and the order parameter vanishes indicating that at the density corresponding to $p_F=0.13\sqrt{\sigma}$, chiral-symmetry restoration occurs.

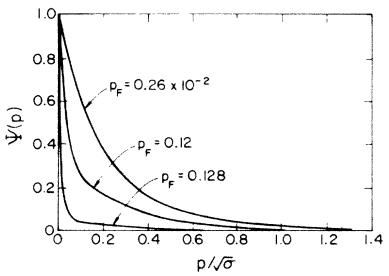

FIG. 6. Gap function vs momentum.

As can be seen from Fig. 7, $\langle\bar{\psi}\psi\rangle$ goes to zero continuously suggesting that the transition is second order. In order to verify this statement, we calculate the ground-state energy difference between the two phases as a function of Fermi momentum. It is easy to calculate the ground-state energy once the propagator is known.[6] In our case it is

$$\delta\epsilon\equiv\epsilon-\epsilon^0 =-N_cn_f\int_p\theta(p-p_F)[(\omega_p+p\cos\phi_p)-(\omega_p^0+p)] , \tag{5.15}$$

where ϵ and ϵ^0 are the ground-state energy densities of the broken and symmetric vacua, respectively. ω_p is the quark energy, Eq. (3.25b), and ω_p^0 is the same quantity evaluated for $\phi_p=0$; i.e., it represents the energy of a massless quark.

Using the gap equation, (5.15) can be rewritten as

$$\delta\epsilon=2N_cn_f\int_p\theta(p-p_F)(\omega_p^0-\omega_p)\left[\frac{1-\cos\phi_p}{2}\right] . \tag{5.16}$$

The behavior of $\delta\epsilon$ as a function of p_F and n is shown in Fig. 8. We see that the only zero of $\delta\epsilon$ is at the critical point indicating that transition is second order.

In Sec. IV the expression for the pion-decay constant was given in Eq. (4.41). Once the gap function is obtained, it is easy to solve Eq. (4.39) for $g(p)$. At zero density

$$g(p)p\cos\phi_p=\sin\phi_p+\frac{C_F}{2}\int_q\tilde{V}(\mathbf{p}-\mathbf{q})(\sin\phi_p\sin\phi_q+\cos\phi_p\cos\phi_q\hat{\mathbf{p}}\cdot\hat{\mathbf{q}})\times[g(q)-g(p)] \tag{5.17}$$

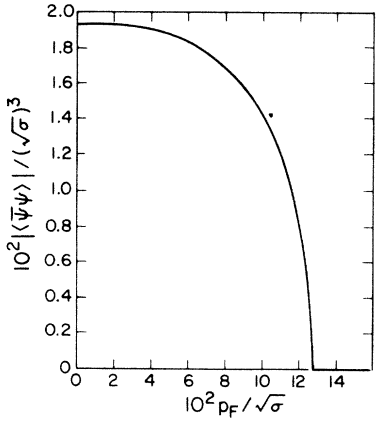

FIG. 7. Order parameter as a function of Fermi momentum.

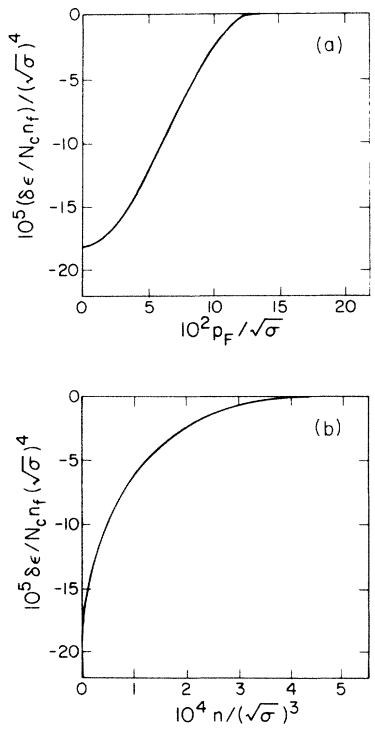

FIG. 8. Energy density difference as a function of (a) Fermi momentum (b) density.

and the pion-decay constant is

$$f_\pi^2 = N_c \int_q \sin\phi_q g(q) \ . \tag{5.18}$$

$g(p)$ is a monotonically decreasing function with its maximum at the origin,[11] and following limiting behavior for large p:

$$g(p) \to \text{const} \times \frac{\tilde{V}(p)}{p^2} \ . \tag{5.19}$$

When the σ dependence is recovered,

$$f_\pi = 0.03\sqrt{\sigma} \ . \tag{5.20}$$

If we attempt to calculate the values of physical quantities, e.g., order parameter and pion-decay constant by adopting the value of σ from charmonium spectroscopy[13] $\sqrt{\sigma}=350$ MeV, we arrive at

$$\langle\bar{\psi}\psi\rangle = (-95 \text{ MeV})^3 \ , \tag{5.21}$$

$$f_\pi = 11 \text{ MeV} \ . \tag{5.22}$$

These values are too small compared to the experimental ones

$$\langle\bar{\psi}\psi\rangle_{\text{expt}} = (-250 \text{ MeV})^3 \ , \tag{5.21a}$$

$$(f_\pi)_{\text{expt}} = 95 \text{ MeV} \ . \tag{5.22a}$$

In addition, the critical Fermi momentum in this case is

$$(p_F)_{\text{crit}} = 0.23 \text{ fm}^{-1} \ . \tag{5.23}$$

This value is totally unacceptable because it is smaller than the Fermi momentum of a nuclear matter

$$(p_F)_{\text{NM}} = 1.34 \text{ fm}^{-1} \ . \tag{5.24}$$

However, this discrepancy is not surprising and we shall argue that it is consistent with our model. In fact, the disagreement of $\langle\bar{\psi}\psi\rangle$ and f_π with experiment indicates that in addition to confining forces, one has to include the short-distance effects of the quark-antiquark interaction in order to obtain the realistic potential in this regime. It is not difficult to show that the presence of the Coulomb potential in the gap equation would produce a considerable enhancement in the values of physical quantities like f_π and $\langle\bar{\psi}\psi\rangle$. From the general behavior of $g(p)$ it is clear that since

$$g(p) \le g(0) < 1 \ , \tag{5.25}$$

it follows that

$$f_\pi^2 \le \frac{g(0)}{2\sqrt{\sigma}} |\langle\bar{\psi}\psi\rangle| \ . \tag{5.26}$$

This equation places an upper limit on f_π and we can examine the influence of a potential upon the order parameter. From the definition of $\langle\bar{\psi}\psi\rangle$ at zero temperature and density

$$\langle\bar{\psi}\psi\rangle = -\frac{N_c}{\pi^2}\int_0^\infty dq\, q^2 \sin\phi_q \ , \tag{5.27}$$

we see that the main contribution to the integral comes from the large and intermediate q's. For a confining potential, the asymptotic form of ϕ_p for large p is

$$\phi_p^{\text{conf}} \to \text{const} \times \frac{1}{p^5} \ . \tag{5.28}$$

The addition of the Coulomb interaction will change this to

$$\phi_p^{\text{coul}} \to \text{const} \times \frac{1}{p^3} \ . \tag{5.29}$$

Renormalization effects[11] will increase the power of p in (5.29) and the overall effect will be the same as if the string tension was increased. Thus, this improved form of potential would produce the higher values of both $\langle\bar{\psi}\psi\rangle$ and f_π. Calculations for a pure Coulomb potential,[7] as well as our analysis of the extreme short-distance potential in Sec. IV confirm these expectations.

As for the value of the critical density, it is useful to examine the density of pairs in the condensate as a function

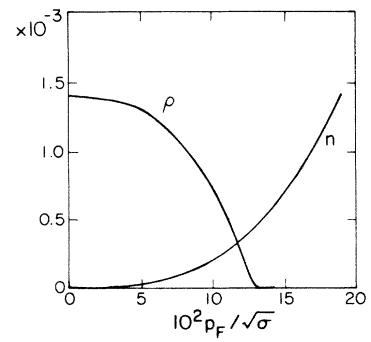

FIG. 9. Density of pairs in the condensate ρ and quark density n vs Fermi momentum.

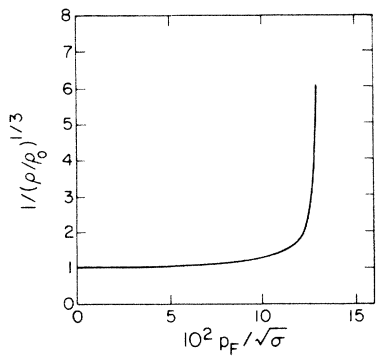

FIG. 10. Average separation between the quarks in a pair $1/\sqrt[3]{\rho}$ in units of $1/\sqrt[3]{\rho_0}$.

of Fermi momentum

$$\rho = 2N_c n_f \int_q \theta(q-p_F)\left[\frac{1-\cos\phi_p}{2}\right] . \tag{5.30}$$

This quantity is a scale parameter associated with the ground state. Its behavior is illustrated in Fig. 9. The average separation between the quarks in a pair is determined by $1/\sqrt[3]{\rho}$ (Fig. 10). If the quarks move on a scale smaller than $1/\sqrt[3]{\rho}$, they do not feel the presence of the condensate and behave as massless. Conversely, at large scales (compared to $1/\sqrt[3]{\rho}$) the symmetry-breaking effects of the ground state make quarks massive. Finite quark density introduces a new scale $1/\sqrt[3]{n}$ which measures the average distance between the surrounding quarks. As the density of surrounding quarks increases, ρ decreases; i.e., the length scale $1/\sqrt[3]{\rho}$ increases. At the point where the two scales become comparable, one expects the theory to regain its underlying chiral symmetry. Our calculations (Fig. 9) support this analysis.

At zero density, ρ has its maximum ρ_0, and for $\sqrt{\sigma}=350$ MeV it is

$$\rho_0 = (39\ \text{MeV})^3 . \tag{5.31}$$

This corresponds to

$$1/\sqrt[3]{\rho} = 5\ \text{fm} . \tag{5.32}$$

This identification of pseudoparticles, defined in Sec. II, with constituent quarks is necessary in order that the hadron spectrum be realized in agreement with the Goldstone theorem and current-algebra predictions. Hence, the hadron radius has to be bigger than $1/\sqrt[3]{\rho}$ and in this model, according to (5.32), it should be at least 5 fm.

The high-density phase transition occurs, essentially, when nucleons begin to overlap. The critical density is roughly

$$n_{\text{crit}} = \frac{1}{\frac{4\pi}{3}R_N{}^3} , \tag{5.33}$$

where R_N is the nucleon radius. Hence

$$(p_F)_{\text{crit}} \sim \frac{1}{R_N} . \tag{5.34}$$

We see that improvements in the model yielding a better value of ρ, and consequently R_N, should enhance $(p_F)_{\text{crit}}$ considerably.

VI. DISCUSSION AND CONCLUSIONS

Using the Schwinger-Dyson equation we studied the effect of finite quark density upon the chiral-symmetry breaking within the pairing model of the QCD vacuum. The presence of quarks amounts to replacing the coupling constant g or σ with the momentum-dependent one, gF_p or σF_p, where $F_p \leq 1$ (Pauli blocking). Two cases were investigated, a δ function and a purely confining potential and in both cases it was found that at finite densities chiral symmetry is restored and the pion decouples. However, the mechanism responsible for the transition is different for the two potentials. For the δ function it was demonstrated that chiral-symmetry breaking occurs if the coupling is bigger than some critical value. Hence, increasing the density, one reduces the coupling, and beyond the critical density, chiral symmetry is restored. Furthermore, this model showed the possible effects of the extreme short-range forces. On the other hand, in the case of a confining potential, Pauli blocking affects the self-energy and eventually stabilizes the symmetric vacuum. Chiral-symmetry restoration occurs without deconfinement. Using the value $\sqrt{\sigma}=350$ MeV one obtains values of physical quantities that are consistently smaller than the experimental ones.

Results for the Coulomb potential presented in Ref. 7 and the extrapolations between the two cases studied in this paper suggest that an adequate potential at intermediate couplings is needed in order to obtain realistic predictions for the critical density as well as for other physical quantities. Inclusion of explicit symmetry-breaking effects, i.e., small quark masses, should make the model more realistic about nuclear physics where it is believed that the pion mass sets the scale.

It is well known that the additive potential models of colored quarks predict an unphysical long-range "color van der Waals" force between hadrons.[14] It would be interesting to see to what extent these forces are affected (screened?) by the presence of the condensate. A first step towards understanding this effect would be the calculation of the effective interaction between constituent quarks. Work on these problems is in progress.

ACKNOWLEDGMENTS

The author wishes to thank Professor J. Kogut for introducing him to the problem of chiral-symmetry breaking and for many useful discussions. Also, discussions with Professor V. Pandharipande are gratefully acknowledged. This work was supported in part by the National Science Foundation under Grant No. NSF PHY 82-01948.

[1]J. Kogut, M. Stone, H. W. Wyld, W. R. Gibbs, J. Shigemitsu, S. H. Shenker, and D. K. Sinclair, Phys. Rev. Lett. **50**, 393 (1983); H. Satz, Nucl. Phys. **A418**, 447c (1984). For a recent review see, J. Cleymans, R. V. Gavai, and E. Suhonen, Phys. Rep. **130**, 217 (1986); E. V. Shuryak, *ibid.* **115**, 151 (1984).

[2]*Statistical Mechanics of Quarks and Hadrons,* edited by H. Satz (North-Holland, Amsterdam, 1981); J. Kogut, H. Matsuoka, M. Stone, H. W. Wyld, S. H. Shenker, J. Shigemitsu, and D. K. Sinclair, Nucl. Phys. **B225**, 93 (1983); B. A. Freedman and L. D. McLerran, Phys. Rev. D **16**, 1130 (1977); **16**, 1147 (1977); **16**, 1169 (1977); J. C. Collins and M. J. Perry, Phys. Rev. Lett. **34**, 1353 (1975).

[3]J. R. Finger and J. E. Mandula, Nucl. Phys. **B199**, 168 (1982); J. R. Finger, J. E. Mandula, and J. Weyers, Phys. Lett. **96B**, 367 (1980).

[4]A. Casher, Phys. Lett. **83B**, 395 (1979).

[5]Y. Nambu and G. Jona-Lasinio, Phys. Rev. **122**, 345 (1961); M. E. Peskin, in *Recent Advances in Field Theory and Statistical Mechanics,* edited by J. B. Zuber and R. Stora (North-Holland, Amsterdam, 1984).

[6]A. Fetter and J. D. Walecka, *Quantum Theory of Many-Particle Systems* (McGraw-Hill, New York, 1971).

[7]J. Govaerts, J. E. Mandula, and J. Weyers, Nucl. Phys. **B237**, 59 (1984); Phys. Lett. **130B**, 427 (1983).

[8]A. C. Davis and A. M. Matheson, Nucl. Phys. **B246**, 203 (1984).

[9]O. Alvarez and R. D. Pisarski, Phys. Rev. D **26**, 3735 (1982).

[10]A. Le Yaouanc, L. Oliver, O. Pene, and J.-C. Raynal, Phys. Rev. Lett. D **29**, 1233 (1984); A. Amer, A. Le Yaouanc, L. Oliver, O. Pene, and J.-C. Raynal, Phys. Rev. Lett. **50**, 87 (1983).

[11]S. L. Adler and A. C. Davis, Nucl. Phys. **B244**, 469 (1984).

[12]S. L. Adler and T. Piran, Rev. Mod. Phys. **56**, 1 (1984).

[13]E. Eichten, K. Gottfried, T. Kinoshita, K. D. Lane, and T. M. Yan, Phys. Rev. D **21**, 203 (1980).

[14]S. Matsuyama and H. Miyazawa, Prog. Theor. Phys. **61**, 942 (1979); O. W. Greenberg and H. J. Lipkin, Nucl. Phys. **A370**, 349 (1981).